International Journal of Applied Mathematics & Statistical Sciences (IJAMSS)
ISSN(P): 2319-3972; ISSN(E): 2319-3980
Vol. 3, Issue 6, Nov 2014, 17-28

International Academy of Science, Engineering and Technology
Connecting Researchers; Nurturing Innovations

THE EFFECT OF HEAT TRANSFER ON TWO-LAYERED BLOOD FLOW THROUGH A COMPOSITE STENOSIS IN THE PRESENCE OF A MAGNETIC FIELD

ALANA R. SANKAR[1], SREEDHARA RAO GUNAKALA[2] & DONNA M. G. COMISSIONG[3]

Department of Mathematics and Statistics, The University of the West Indies, Trinidad and Tobago

ABSTRACT

A two layered model consisting of a peripheral cell-free layer and a core particle-fluid suspension was used to describe blood flow through a composite stenosis in the presence of both an external magnetic field and convective heat transfer. The effect of varying the strength of the magnetic field and the pressure gradient on the fluid's velocity was examined. Temperature profiles were generated and used to examine the effect of varying the magnetic field strength and hematocrit level on blood temperature. The effect of varying the magnetic field strength, hematocrit and stenosis height on the friction-factor Reynold's number and Nusselt number was examined in the presence of the composite stenosis. This knowledge can aid in the improvement of existing diagnostic tools used for cardiovascular diseases and in the understanding of the effect that a magnetic field and convective heat will have on cardiovascular patients.

KEYWORDS: Blood Flow, Heat Transfer, Hematocrit, Magnetic Field, Stenosis

INTRODUCTION

Cardiovascular disease is expected to remain a popular subject of scientific research and the single leading cause of death worldwide according to the World Health Organisation's prediction of 23.3 million deaths by 2030 [1]. The two major events that contribute to these deaths are the occurence of a heart attack or a stroke. These usually follow a blockage in the blood flow to the heart or the brain respectively by a stenosis. A stenosis is an abnormal growth which can form at any location of the cardiovascular system under diseased conditions. It can be modelled as a single (bell-shaped, symmetric, non-symmetric, composite) or a multiple (overlapping, irregularly shaped) stenosis. The study of a composite stenosis is important since the shape of the stenosis in the artery varies. Blood flow studies involving magnetic effects and heat transfer can provide useful insights into the diagnostics of cardiovascular diseases.

Blood circulation has a vital role to play in the heat transfer between living tissues, especially in the peripheral vessels where the temperature is closely related to the blood flow rate. Although the outer surface of the human skin can tolerate and adapt to large temperature changes, the human internal organs cannot. When the temperature changes, a sophisticated heat regulatory system is necessary to facilitate heat loss or heat gain to keep the internal body temperature around 98.6^0F [2]. Body heat that is produced by the skeletal muscles is removed by convective heat transfer. Convection is heat transfer which is accomplished by mass transfer i.e. movement in the fluid. If the fluid motion involved in the process is induced by some external means (e.g. pump, blower, wind, vehicle motion, etc.) the process is called forced convection [3]. Since human blood is pumped by the heart, forced convection is a suitable model for heat transfer. Wang studied the forced convection heat transfer in a narrow vessel using a two fluid model [4]. Sanyal et al. extended this model to include the effects of a magnetic field. Convective thermodynamic studies are significant to processes like oxygenation and haemodialysis but can also be applied to the study of local hyperthermia and cryosurgery for tumour treatment [5].

The thermally important blood vessels are the ones with diameters ranging between 50-500 μm since these smaller blood vessels were observed to be more actively engaged in heat exchange. To realistically describe blood flow in blood vessels of diameter ≤ 1000 μm, based on Haynes' theoretical analysis and Cokelet's experimental observations, a single-phase fluid analysis is insufficient [6, 7]. Further, the discovery that hematocrit (red cell volume fraction) in human blood is approximately 45% and has a strong influence on the blood flow properties of blood led to the treatment of the red blood cells (erythrocytes) as discrete particles [8]. Thus, the two-phase macroscopic model (i.e. a suspension of red cells in plasma) proposed by Srivastava and Srivastava for blood flow in small vessels (of diameter ≤ 2400 μm) catered for the individuality of the red cells (of diameter 8 μm) [9]. Additionally, experimental work provided evidence for the existence of a layer of plasma containing no cells located layer near the walls and a core region containing all the erythrocytes suspended in plasma [10]. Therefore a two layered model consisting of a cell free peripheral plasma layer and a core region with the red blood cells in plasma can be used to more realistically describe blood flow in these thermally important vessels.

Using this two-layered model Sankar et al. examined the effect that an external, uniform, transverse magnetic field had on the blood's velocity, flow rate and three of its flow characteristics through a composite stenosis [11]. Low intensity, low frequency magnetic energy is used to treat chronic pain secondary to tissue ischemia and non healing or slowly healing ulcers. In this study however, the effects of heat transfer will be included by considering forced convective heat transfer. A more realistic two-layered flow consisting of a peripheral cell-free layer and a core two-phase flow in the presence of a composite stenosis was utilised. Convective heat transfer in the presence of a stenosis has not been studied previously. Also the effect of convective heat transfer on the chosen mathematical model has not been examined in the previous literature. From this study, velocity and temperature profiles will be generated and the effect of the magnetic field, hematocrit and stenosis height on the friction-factor Reynold's number and Nusselt number will be examined in the presence of the stenosis.

METHODOLOGY

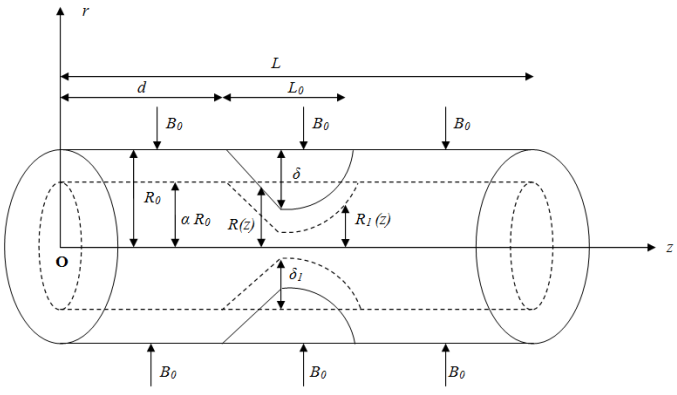

Figure 1: The Geometry of the Stenosed Artery

Consider a two layered model for the axisymmetrical, fully developed, steady, laminar flow of blood through a cylindrical vessel in the presence of a composite stenosis. The two layers are a central core layer of radius R_1 which is a suspension of red blood cells (erythrocytes) in plasma and a peripheral plasma layer of thickness $(R - R_1)$ modelled as a Newtonian, viscous fluid. The wall near to the stenosis development is assumed to be solid. The artery is assumed to be

uniform, circular and rigid with its length being much greater than its radius so that entrance, end and special wall effects can be neglected. A uniform, transverse magnetic field is applied in the axial direction in the presence of forced convective heat transfer. The geometry of the stenosis that is manifested in the arterial segment is described in Figure 1 as [12, 13].

$$\frac{(R(z),R_1(z))}{R_0} = (1,\alpha) - \frac{2}{R_0 L_0}(\delta,\delta_1)(z-d);\ d \le z \le d + \frac{L_0}{2}$$

$$= (1,\alpha) - \frac{(\delta,\delta_1)}{2R_0}\left[1 + \cos\frac{2\pi}{L_0}\left(z - d - \frac{L_0}{2}\right)\right];\ d + \frac{L_0}{2} \le z \le d + L_0$$

$$= (1,\alpha);\ \text{otherwise}$$

where R_0 are the radius of the tube without any constriction and $R \cong R(z)$ is the radius of the tube with constriction. The length of the tube is denoted by L and the length of the stenosis by L_0. The stenosis starts at $z = d$. In the unobstructed region, the ratio of the radius of the central core to that of the tube is α. The maximum height of the stenosis and bulging of the interface at the location where $z = d + \frac{L_0}{2}$ in the stenotic region is (δ,δ_1).

In the core region, $(0 \le r \le R_1)$ in the presence of Lorentz's force a two-phase macroscopic model is used with the following governing equations [9, 13].

For the fluid (plasma) phase:

Equations of axial and radial momentum

$$(1-C)\rho_f\left(\frac{\partial u_f}{\partial t} + u_f\frac{\partial u_f}{\partial z} + v_f\frac{\partial u_f}{\partial r}\right) = -(1-C)\frac{\partial p}{\partial z} + (1-C)\mu_s(C)\nabla^2 u_f + CS(u_p - u_f) - \sigma B_0^2 u_f, \tag{1}$$

$$(1-C)\rho_f\left(\frac{\partial v_f}{\partial t} + u_f\frac{\partial v_f}{\partial z} + v_f\frac{\partial v_f}{\partial r}\right) = -(1-C)\frac{\partial p}{\partial r} + (1-C)\mu_s(C)\left(\nabla^2 - \frac{1}{r^2}\right)v_f + CS(v_p - v_f). \tag{2}$$

Equation of continuity

$$\frac{1}{r}\frac{\partial}{\partial r}\left[r(1-C)v_f\right] + \frac{\partial}{\partial z}\left[(1-C)u_f\right] = 0. \tag{3}$$

For the particle (erythrocyte) phase:

Equations of axial and radial momentum

$$C\rho_p\left(\frac{\partial u_p}{\partial t} + u_p\frac{\partial u_p}{\partial z} + v_p\frac{\partial u_p}{\partial r}\right) = -C\frac{\partial p}{\partial z} + CS(u_f - u_p), \tag{4}$$

$$C\rho_p\left(\frac{\partial v_p}{\partial t} + u_p\frac{\partial v_p}{\partial z} + v_p\frac{\partial v_p}{\partial r}\right) = -C\frac{\partial p}{\partial r} + CS(v_f - v_p). \tag{5}$$

Equation of continuity

$$\frac{1}{r}\frac{\partial}{\partial r}\left(rCv_p\right)+\frac{\partial}{\partial z}\left(Cu_p\right)=0. \tag{6}$$

Here (r,z) are two-dimensional cylindrical polar coordinates with z measured along the axis of the tube and r measured normal to the tube axis, $\nabla^2=\frac{1}{r}\frac{\partial}{\partial r}\left(r\frac{\partial}{\partial r}\right)+\frac{\partial^2}{\partial z^2}$ is a two-dimensional Laplacian operator, (u_f,v_f) and (u_p,v_p) are the (axial, radial) components of the fluid and particle velocities. The volume fraction density of the particles is denoted by C, the pressure by p, μ_0 is the fluid viscosity (suspending medium), the mixture viscosity (apparent or effective viscosity) by $\mu_S(C)\cong\mu_S$, the drag coefficient of interaction for the force exerted by one phase on the other by S with ρ_f and ρ_p are the actual densities of the material constituting the fluid (plasma) and the particle (erythrocytes) phases respectively. The electrical conductivity of the fluid is σ and B_0 is the component of the constant uniform magnetic field which was applied in the axial direction.

The suspension viscosity, μ_s, was chosen from the experimental observations of Charm and Kurland and the drag coefficient of interaction, S, from the classical Stokes drag was modified to account for the finite particulate fractional volume [14, 15].

In the peripheral region, $R_1\le r\le R$, Navier-Stokes equations were used in the presence of the Lorentz's force:

$$\rho_0\left(\frac{\partial u_0}{\partial t}+u_0\frac{\partial u_0}{\partial z}+v_0\frac{\partial u_0}{\partial r}\right)=-\frac{\partial p}{\partial z}+\mu_0\nabla^2u_0-\sigma B_0^2u_0 \tag{7}$$

$$\rho_0\left(\frac{\partial v_0}{\partial t}+u_0\frac{\partial v_0}{\partial z}+v_0\frac{\partial v_0}{\partial r}\right)=-\frac{\partial p}{\partial r}+\mu_0\left(\nabla^2-\frac{1}{r^2}\right)v_0 \tag{8}$$

where (u_0,v_0) are the (axial, radial) components and ρ_0 and the density of the fluid.

The boundary conditions are given as

$$u_0=0,\ \text{at}\ r=R,$$
$$u_0=u_f\ \text{and}\ \tau_p=\tau_f,\ \text{at}\ r=R_1,$$
$$\frac{\partial u_f}{\partial r}=\frac{\partial u_p}{\partial r}=0\ \text{and}\ \tau_f=0,\ \text{at}\ r=0,$$

where $\tau_p=-\mu_0\frac{\partial u_0}{\partial r}$ and $\tau_f=-(1-C)\mu_s\frac{\partial u_f}{\partial r}$ are the shear stresses of the peripheral and central regions respectively [16].

Assuming T_f and T_0 as the temperature on the core and peripheral plasma layer regions respectively and q as the constant heat flux applied on the wall, the following are the forced convection equations.

Equation in core region:

$$\rho_f c_p u_f \frac{\partial T_i}{\partial z} = \frac{k_f}{r}\frac{\partial}{\partial r}\left(r\frac{\partial T_i}{\partial r}\right). \tag{9}$$

Equation in peripheral plasma region:

$$\rho_0 c_p u_0 \frac{\partial T_0}{\partial z} = \frac{k_0}{r}\frac{\partial}{\partial r}\left(r\frac{\partial T_0}{\partial r}\right), \tag{10}$$

where k_0 and k_f are the thermal conductivities in the peripheral plasma layer and core region respectively.

The mean velocity, V, and the mean temperature, T_m, are given as

$$V = 2\left\{\int_{R_1}^{R} r u_0 dr + \int_0^{R_1} r\left[(1-C)u_f + Cu_p\right]dr\right\}, \tag{11}$$

$$T_m = \frac{2}{V}\left\{\int_0^{R_1} u_f T_i r\, dr \int_{R_1}^{R} u_0 T_0 r\, dr\right\}. \tag{12}$$

For constant flows, all temperatures have the same, constant gradient (denoted by G) in the axial direction, that is

$$\frac{\partial T_i}{\partial z} = \frac{\partial T_0}{\partial z} = \frac{\partial T_m}{\partial z} = G. \tag{13}$$

The boundary conditions for the temperatures are given as

$$\begin{gathered} T_i \text{ is bounded at } r = 0, \\ T_0 = T_i \text{ and } k_f \frac{\partial T_i}{\partial r} = k_0 \frac{\partial T_0}{\partial r} \text{ at } r = R_1, \\ k_0 \frac{\partial T_0}{\partial r} = q \quad \text{at } r = R, \\ T_m = 0 \text{ at } z = 0. \end{gathered}$$

RESULTS

After non-dimensionalising using the appropriate non-dimensional variable the following equations are obtained

$$\frac{dp}{dz} = \frac{1}{r}\frac{\partial}{\partial r}\left(r\frac{\partial}{\partial r}\right)u_0 - M^2 u_0, \quad R_1 \le r \le R \tag{14}$$

$$(1-C)\frac{dp}{dz} = (1-C)\frac{\mu_s(C)}{r}\frac{\partial}{\partial r}\left(r\frac{\partial}{\partial r}\right)u_f + CS(u_p - u_f) - M^2 u_f, \; 0 \le r \le R_1, \tag{15}$$

$$C\frac{dp}{dz} = CS(u_f - u_p),\ 0 \le r \le R_1, \tag{16}$$

subjected to

$$u_0 = 0,\ \text{at}\ r = R\ . \tag{17}$$

$$u_0 = u_f \ \text{and}\ \frac{\partial u_0}{\partial r} = (1-C)\mu_s \frac{\partial u_f}{\partial r},\ \text{at}\ r = R_1, \tag{18}$$

$$\frac{\partial u_f}{\partial r} = \frac{\partial u_p}{\partial r} = 0,\ \text{at}\ r = 0, \tag{19}$$

in the presence of a composite stenosis given by

$$\begin{aligned}(R(z), R_1(z)) &= (1, \alpha) - \frac{2}{L_0}(\delta, \delta_1)(z-d);\ d \le z \le d + \frac{L_0}{2} \\ &= (1, \alpha) - \frac{(\delta, \delta_1)}{2}\left[1 + \cos\frac{2\pi}{L_0}\left(z - d - \frac{L_0}{2}\right)\right];\ d + \frac{L_0}{2} \le z \le d + L_0 \\ &= (1, \alpha);\ \text{otherwise}\end{aligned}$$

where M is the Hartmann number.

The expressions for velocities, u_0, u_f and u_p are found to be

$$u_0 = k_1 I_0(Mr) + k_2 K_0(Mr) - \frac{1}{M^2}\left(\frac{dp}{dz}\right),\ R_1 \le r \le R, \tag{20}$$

$$u_f = k_3 J_0(M\gamma r) - \frac{1}{M^2}\left(\frac{dp}{dz}\right),\ 0 \le r \le R_1, \tag{21}$$

$$u_p = k_3 J_0(M\gamma r) - \left(\frac{1}{M^2} + \frac{1}{S}\right)\left(\frac{dp}{dz}\right),\ 0 \le r \le R_1, \tag{22}$$

where

$$k_1 = \frac{\frac{1}{M^2}\left(\frac{dp}{dz}\right) - k_2 K_0(MR)}{I_0(MR)},\quad k_2 = \frac{\frac{1}{M^2}\left(\frac{dp}{dz}\right)\left[I_0(MR_1)(1-C)\mu_s\gamma J_1(M\gamma R_1) + I_1(MR_1)J_0(M\gamma R_1)\right]}{\left\{\begin{array}{l} I_0(MR)[J_0(M\gamma R_1)K_1(MR_1) - K_0(MR_1)(1-C)\mu_s\gamma J_1(M\gamma R_1)] \\ + K_0(MR)[I_0(MR_1)(1-C)\mu_s\gamma J_1(M\gamma R_1) + I_1(MR_1)J_0(M\gamma R_1)]\end{array}\right\}},$$

$$k_3 = \frac{k_2 K_1(MR_1) - k_1 I_1(MR_1)}{(1-C)\mu_s\gamma J_1(M\gamma R_1)} \ \text{and}\ \ \gamma = \sqrt{\frac{1}{(C-1)\mu_s}}$$

where J_n is the Bessel functions of first kind of order n, I_n is the modified Bessel function of the first kind of order n, and K_n is the modified Bessel function of the second kind of order n [11].

The mean velocity, V, is now calculated as

$$V = 2\left\{\frac{k_1}{M}(RI_1(MR) - R_1I_1(MR_1)) + \frac{k_2}{M}(R_1K_1(MR_1) - RK_1(MR)) + \frac{k_3}{M\gamma}(R_1J_1(M\gamma R_1) - \Phi\left(\frac{R^2}{2M^2} + \frac{CR_1^2}{2S}\right)\right\} \text{ where } \Phi = \frac{dp}{dz}. \quad (23)$$

Non-dimensionalising Eq. (9) and Eq.(10) leads to

$$P_c u_f \frac{\partial T_i}{\partial z} = \frac{1}{r}\frac{\partial}{\partial r}\left(r\frac{\partial T_i}{\partial r}\right), \ 0 \le r \le R_1, \quad (24)$$

$$\beta P_c u_0 \frac{\partial T_0}{\partial z} = \frac{1}{r}\frac{\partial}{\partial r}\left(r\frac{\partial T_0}{\partial r}\right), \ R_1 \le r \le R, \quad (25)$$

subjected to

$$T_i \text{ is bounded at } r = 0,$$
$$T_0 = T_i \text{ and } \psi\frac{\partial T_i}{\partial r} = \frac{\partial T_0}{\partial r} \text{ at } r = R_1,$$
$$\frac{\partial T_0}{\partial r} = \psi \quad \text{at } r = R,$$
$$T_m = 0 \text{ at } z = 0,$$

where $\beta = \left(\frac{\kappa_f}{\kappa_0}\right)$ is the ratio of the diffusitivities, $\psi = \left(\frac{k_f}{k_0}\right)$ the ratio of conductivities and P_c the Péclet number.

The expressions found for the temperatures were used to obtain the friction-factor-Reynolds number product, fRe

$$fRe = \frac{8}{V} = \frac{8}{2\left\{\frac{k_1}{M}(RI_1(MR) - R_1I_1(MR_1)) + \frac{k_2}{M}(R_1K_1(MR_1) - RK_1(MR)) + \frac{k_3}{M\gamma}(R_1J_1(M\gamma R_1) - \Phi\left(\frac{R^2}{2M^2} + \frac{CR_1^2}{2S}\right)\right\}}$$

and the Nusselt number, Nu, which is used to gauge the heat transfer to the blood

$$Nu = \frac{2}{T_0(R,z) - T_m(z)}.$$

DISCUSSIONS

Plots of the solutions obtained are provided for the following parameter values: d =0; L_0 =1; C =0, 0.1, 0.2, 0.3, 0.4, 0.5, 0.6; δ =0, 0.05, 0.10, 0.15, M =0, 2, 4, 6, 8, 10. The Péclet number is assumed to be 0.03 for a microvascular

flow [17]. The parameter α is computed using $\alpha = 1 - \varepsilon / R_0$ in which $\varepsilon \cong \varepsilon(C)$ represents the peripheral layer of thickness as a function of cell concentration. In order for the computation to be done, the temperature was chosen as T =25.5 ^{0}C, to be able to use Haynes' analysis where $\varepsilon(\mu m)$ = 6.18, 4.67, 3.60, 3.12, 2.58, 2.18 corresponds to hematocrit (%) =10, 20, 30, 40, 50, 60 respectively [6]. Simpson's rule is used to evaluate any integral which needed to be solved numerically.

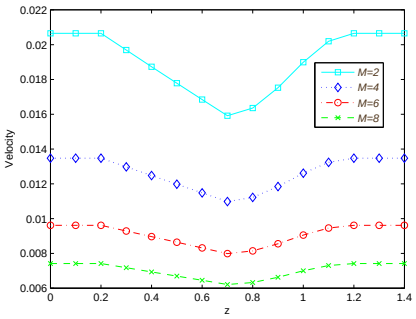

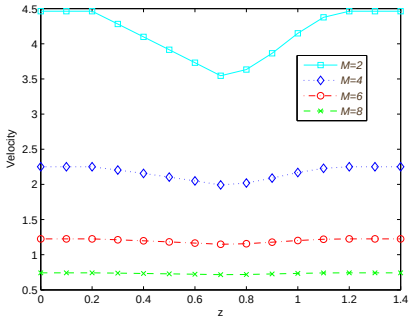

Figure 2(a) **Figure 2(b)**

Figure 2: The Effect of Varying the Hartmann Number, M , on The Fluid's Velocity in the (a) Peripheral Region at $r = \frac{(\alpha+1)R}{2}$ and (b) Core Region at $r = \frac{R_1}{2}$

The velocity profiles in Figures 2(a) and 2(b), show that as the Hartmann number increases, the velocity of the fluid decreases in the both layers of the flow. This reduction in the fluid's velocity is due to the opposing Lorentz's force that is introduced when the magnetic field is applied. This trend was also observed by Sankar et al. [11]. The velocity of the fluid in the core region is larger than that in the peripheral region. There is a decrease in the velocity of the flow in the upstream of the stenosis and a gradual increase in its downstream in the both regions.

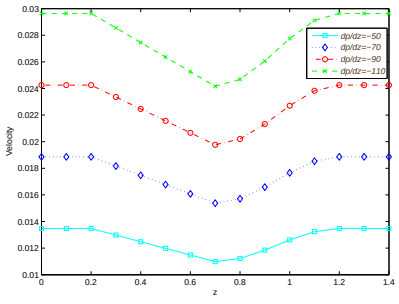

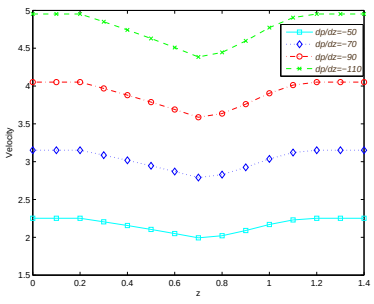

Figure 3(a) **Figure 3(b)**

Figure 3: The Effect of Varying the Pressure Gradient, $\frac{dp}{dz}$, on the Fluid's Velocity in the (a) Peripheral Region at $r = \frac{(\alpha+1)R}{2}$ and (b) Core Region at $r = \frac{R_1}{2}$.

The velocity profiles given in Figures 3(a) and 3(b) show that as the pressure gradient, $\frac{dp}{dz}$, increases, the velocity of the fluid increases in both layers of the flow. Therefore the higher the pressure gradient of the flow, the faster the blood will flow through the blood vessel.

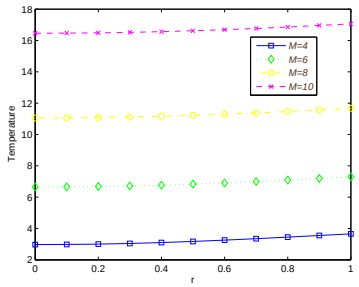

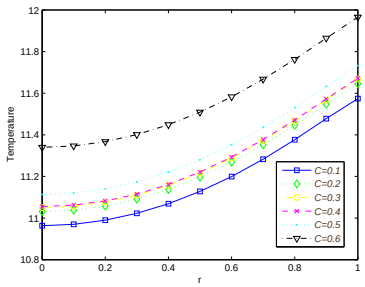

Figure 4(a) **Figure 4(b)**

Figure 4: Variation of Temperature with Changes in (a) Hartmann Number, M ($C = 0.4, \beta = \psi = 1, P_c = 0.03$) and (b) Hematocrit, C ($M = 8, \beta = \psi = 1, P_c = 0.03$)

Now on the introduction of convective heat transfer, the following temperature profiles shown in Figures 4(a) and 4(b) are obtained. From Figure 4(a), as the Hartmann number, M, increased the temperature increased. Thus the temperature of the blood can be increased when needed by the introduction of the certain magnetic field strength. This is the primary objective of hyperthermia in cancer therapy whereby the temperature is raised above cytotoxic temperature (41-45^{0}C) without over exposing healthy tissues [18]. From Figure 4(b), it can be noted that as the hematocrit, C, increases, the temperature increases.

Both the friction-factor-Reynolds number product and Nusselt number were computed and plotted varying different parameters. In general, fRe increased in the upstream of the stenosis growth and reached its maximum at the point where the stenosis height was at its greatest and then decreased downstream. There was a general decrease in Nu as the flow progressed.

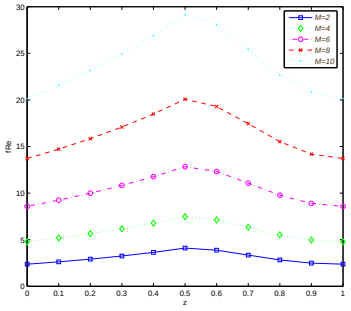

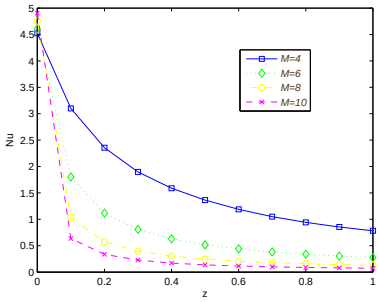

Figure 5(a) **Figure 5(b)**

Figure 5: The Effect of Varying The Hartmann Number, M, On (a) fRe ($C = 0.4, \delta = 0.15$) and (b) Nu ($C = 0.2, \beta = \psi = 1, P_c = 0.03, \delta = 0.1$).

The trend observed in Figure 5(a), where fRe increased as M increased is in keeping with Sanyal et al. [5]. This occurred because as M increased, the velocity decreased, so the friction-factor-Reynolds number product was expected to increase. From Figure 5(b), for a low Péclet number, as the Hartmann number increased, the Nusselt number decreased. This trend as also observed in another blood flow study by Chaturvedi et al. [2].

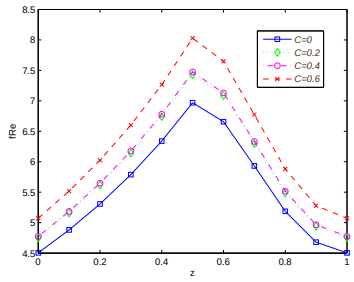

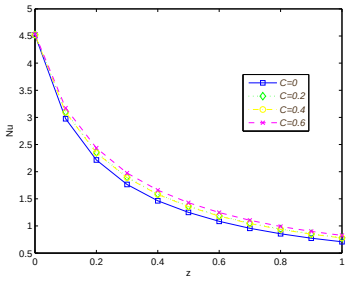

Figure 6(a) **Figure 6(b)**

Figure 6: The Effect of Varying The Hematocrit, C , on (a) fRe $(M = 4,\ \delta = 0.15)$ and (b) Nu $(M = 4, \beta = \psi = 1, P_C = 0.03, \delta = 0.1)$.

With increasing hematocrit both the friction-factor-Reynolds number product and Nusselt number increased (see Figures 6(a) and 6(b)). That is, in the presence of a high number of red blood cells, there would be a greater heat and energy loss taking place. This is important to predict the effect this will have on the blood flow in patients with plasma cell dyscrasias (hematocrit=28.00%, α =0.816), Hb SS-sickle cell (hematocrit=24.80%, α =0.795), hypertension-controlled (hematocrit=43.13%, α =0.928), hypertension-uncontrolled (hematocrit=43.25%, α =0.925) and polycythemia (hematocrit=63.20%, α =0.990) in which the hematocrit level varies [10].

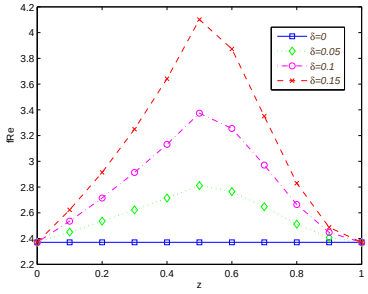

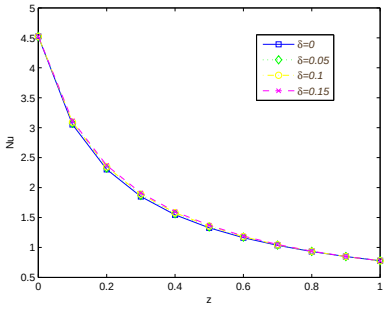

Figure 7(a) **Figure 7(b)**

Figure 7: The Effect of Varying The Stenosis Height, δ , on (a) fRe $(C = 0.4, M = 2)$ and (b) Nu $(M = 4, \beta = \psi = 1, P_C = 0.03, C = 0.4)$.

From Figures 7(a) and 7(b), it was observed that as the stenosis height increased, the friction-factor-Reynolds number product increased and there was a very small increase in the Nusselt number. This can be useful in the analysis of heat transfer in patients with atherosclerotic plaque. As the atherosclerotic plaque growth progresses, if the patient is exposed to heat, it can be predicted that there would be a greater energy loss and a greater heat loss taking place in the blood.

CONCLUSIONS

The velocity of the fluid decreased as the Hartmann number increased due to the opposing Lorentz's force which increases as the magnetic field strengthens. There was a decrease in the velocity of the flow in the upstream of the stenosis and the a gradual increase in its downstream. As the pressure gradient increased the velocity also increased. In the presence of convective heat transfer, the temperature of the blood increased when the Hartman number increased. As hematocrit increased, temperature increased, and both the friction-factor Reynolds number product and Nusselt number increased.

The friction-factor Reynolds number product and Nusselt number also increased as the stenosis height increased. As the Hartmann number increased, that is as the strength of the magnetic field is increased, the friction-factor Reynolds number product increased and the Nusselt number decreased. The restrictions present in this study (including the rigid wall, steady and fully developed flow, constant thickness of the peripheral layer) did not prevent it from being useful in understanding the flow phenomena.

In conclusion, magnetic fields can be beneficial in reducing blood velocity and increasing blood temperature if needed. The effects of heat transfer on blood flow in the presence of a stenosis can be predicted by examining the effect that varying the hematocrit and stenosis height had on the friction-factor Reynolds number product and the Nusselt number. This can be especially beneficial for predicting the effect of convective heat on persons with blood conditions in which the hematocrit level varies and in atherosclerosis patients. Studies on two layered flows are not only important to the understanding of physiological flows (blood flow, protein diffusion, microorganisms movement, particle deposition on the respiratory tract) but also to other areas of research such as powder technology, petroleum transport, aerosol filtration, waste water treatment, fluidization, mining, power plant piping, corrosive particles in engine oil flow, environmental pollution, lunar ash flows, atmospheric fallout, combustion, agriculture and food technologies.

REFERENCES

1. World Health Organisation, “Cardiovascular diseases (CVDs).” 2013 [Online]. Available: http://www.who.int/mediacentre/factsheets/fs317/en/index.html. [Accessed: Oct. 15, 2013].
2. R. Chaturvedi, R. K. Srivastav and Vinay Kumar Jadon, Blood Flow in Presence of Magnetic field through porous medium and its effects on heat transfer rate. International Journal of Advanced Computer and Mathematical Sciences, 3(2)(2012) 266-271.
3. P. S. Ghoshdastidar, Heat Transfer, Oxford University Press, New York, (2004).
4. C. Y. Wang, Heat transfer to Blood Flow in a Small tube, Journal of Biomedical Engineering, 130(2008) 1-3.
5. D. C. Sanyal, K. Das, and S. Debnath, Heat transfer in a Two-layered Blood Flow Model in a Narrow tube in presence of Magnetic field, African Journal of Mathematical Physics, 7(2009) 1-8.
6. R. Haynes, Physical basis of the dependence of blood viscosity on tube radius, American Journal of Physiology, 198(1960) 1193-1205.
7. G. R. Cokelet, The Rheology of Human Blood: In Biomechanics, Prentice-Hall, New Jersey, Englewood Cliffs, (1972).
8. R. Skalak, Mechanics of microcirculation: In Biomechanics, Its Foundation and Objectives, New Jersey, Prentice-Hall, Englewood Cliffs, (1972).
9. L. Srivastava and V. Srivastava, On two-phase model of pulsatile blood flow with entrance effects, Biorheology, 20(1983) 761-777.
10. G. Bugliarello and J. Sevilla, Velocity distribution and other characteristics of Steady and Pulsatile Blood Flow in fine glass tubes, Biorheology, 7(1970) 85-107.
11. A. Sankar, S. R. Gunakala and D. M. G. Comissiong, Two-layered Blood flow through a Composite Stenosis in

the Presence of a Magnetic Field, International Journal of Application of Innovation in Engineering and Management, 2 (12)(2013), 30-41.

12. P. Joshi, A. Pathak and B. Joshi, Two-layered model of blood flow through composite stenosed artery, Applications and Applied Mathematics, 4(2009), 343-354.
13. A. Sankar, S. R. Gunakala and D. M. G. Comissiong, Two-Layered Suspension Blood Flow Through a Composite Stenosis, Journal of Mathematics Research, 5(4)(2013), 26-38.
14. S. Charm and G. Kurland, Blood flow and Microcirculation, New York, John Wiley, (1974).
15. C. Tam, The drag on a cloud of spherical particles in low Reynolds number flows, Journal of Fluid Mechanics, 38(1969), 537-546.
16. V. Srivastava and M. Saxena, Suspension model for blood flow through stenotic arteries with a cell-free plasma layer, Mathematical Biosciences, 139(1997), 79-102.
17. M. Zakharov and M. Sadovsky, The role of blood circulatory system in thermal regulation of animals explained by entropy production analysis, arXiv: 1308. 3663 [q-bio. OT]
18. J. Overgaad and D. Gonzalez, M. C. C. H Hulshof, G. Arcangeli, O. Dahl, O. Mella, and S. M. Bentzen, Hyperthermia as an adjuvant to radiation therapy of recurrent or metastatic melanoma: a multicenter randomized trial by the European Society for Hyperthermia Oncology, International Journal of Hyperthermia, 12 (1)(1996), 3-20.